OPEN

Low-Field Magnetic Resonance Imaging
Its History and Renaissance

Masaaki Hori, MD, PhD,*† Akifumi Hagiwara, MD, PhD,† Masami Goto, PhD,‡
Akihiko Wada, MD, PhD,† and Shigeki Aoki, MD, PhD†

Abstract: Low-field magnetic resonance imaging (MRI) systems have seen a renaissance recently due to improvements in technology (both hardware and software). Originally, the performance of low-field MRI systems was rated lower than their actual clinical usefulness, and they were viewed as low-cost but poorly performing systems. However, various applications similar to high-field MRI systems (1.5 T and 3 T) have gradually become possible, culminating with high-performance low-field MRI systems and their adaptations now being proposed that have unique advantages over high-field MRI systems in various aspects. This review article describes the physical characteristics of low-field MRI systems and presents both their advantages and disadvantages for clinical use (past to present), along with their cutting-edge clinical applications.

Key Words: magnetic resonance imaging, low-field MRI, clinical applications

This review focuses on low-field magnetic resonance imaging (MRI) systems. Low-field MRI systems (generally defined as systems in the range 0.25–1.0 T)[1] have traditionally been viewed as poorly performing systems because the older types of low-field MRI systems often had limited spatial resolution associated with poor image quality, limited available receiver coils, limited kinds of image sequences and parameters, and inefficient temporal resolution associated with low signal-to-noise ratio (SNR).[2] In fact, in the 1980s, when many low-field MRI systems were in widespread clinical use, there was a perception in the scientific community that higher static field strengths would enable higher performance MRI.[1] This led to comparison studies being conducted with various MRIs at different static field strengths. The results obtained confirmed the improvement in image quality at higher fields.[3–9] In MRI systems, the most basic way to achieve a higher SNR is to increase the static magnetic field strength. This is because the MRI signal itself is proportional to the square of the static magnetic field strength, and the noise is proportional to the static magnetic field strength. Based on these principles, a 3-T MR system can theoretically achieve 15 times the SNR of a 0.2-T MRI system.[10] Moreover, to improve SNR, it is self-evident that significant investments (in terms of effort and financial capital) by researchers and

scientists in hardware with increased gradient strengths/slew rates and stability are necessary.[1] The initially developed clinical MRI systems had magnetic field strengths of 0.35 T and less. Various advancements have since been made in this area. One of these advancements is the improvement of the static magnetic field over the past 40 years, with 1.5-T and 3-T MRI now becoming the main MRI systems for clinical use, replacing the old low-field MRI systems.[1] The history of the evolution of the field strength of clinical MR systems has been discussed in detail by Runge and Heverhagen.[11]

However, the concept of direct SNR dependence on magnetic field strength has since been determined to be false.[12–14] This is because the static magnetic field strength alone does not determine the image SNR, and advances (since the late 1990s) in software (including various sequences) and hardware (including gradients and imaging coils) have made balanced sequences and high-speed contrast-enhanced MR angiography (MRA) possible in low-field systems. In the past, imaging sequences for low-field MRI systems were relatively limited and basic, but now they have become quite sophisticated and are comparable to the imaging sequences of 1.5-T MRI systems that are widely used clinically. In addition, the low SNR inherent in low-field MRI systems has been improved by image reconstruction methods using deep learning and denoising techniques. This has resulted in high image quality that is sufficient for clinical applications.[15–20] Considering these factors, low-field MRI systems can be expected to become very popular tools in regions of the world where MRI is difficult to install or access owing to cost, especially in terms of maintenance.[21–23] In addition, another clear benefit of low-field systems is the reduced weight of the systems, perhaps even facilitating mobility.[2]

However, it is important to understand that low-field MRI systems are different from 1.5-T or 3-T MRI systems, which are the backbone and accepted standard of the MRI technique and scanner configuration. The so-called physical characteristics (eg, differences in longitudinal relaxation [T1] values and chemical shifts) will cause image differences that cannot be altered by the aforementioned deep learning techniques. It is critical to understand these differences before imaging. Nonetheless, despite these differences, a low static magnetic field strength can be advantageous.

In this review, we discuss both the advantages and drawbacks of low-field MRI systems.

PHYSICAL CHARACTERISTICS OF LOW-FIELD MAGNETIC RESONANCE IMAGING SYSTEMS

The average chemical shift difference between protons in fat and water is approximately 3.5 ppm at any field strength MRI system.[24,25] Therefore, protons in fat have a resonance frequency difference of 224 Hz at 1.5-T MRI and 22 Hz at 0.15-T MRI.[25] This chemical shift is useful for detecting small fatty components in lesions and has been used clinically in adrenal gland[26] and bone and soft tissue lesions.[27] However, it can cause chemical shift artifacts in clinical imaging in MRI that can become a major problem at higher static field strengths.[28] The chemical shifts of these artifacts are inversely proportional to the sampling bandwidth. Thus, as a solution, it is possible to increase the bandwidth and suppress chemical shift artifacts within an acceptable SNR range because the original SNR response of high-field MRI systems
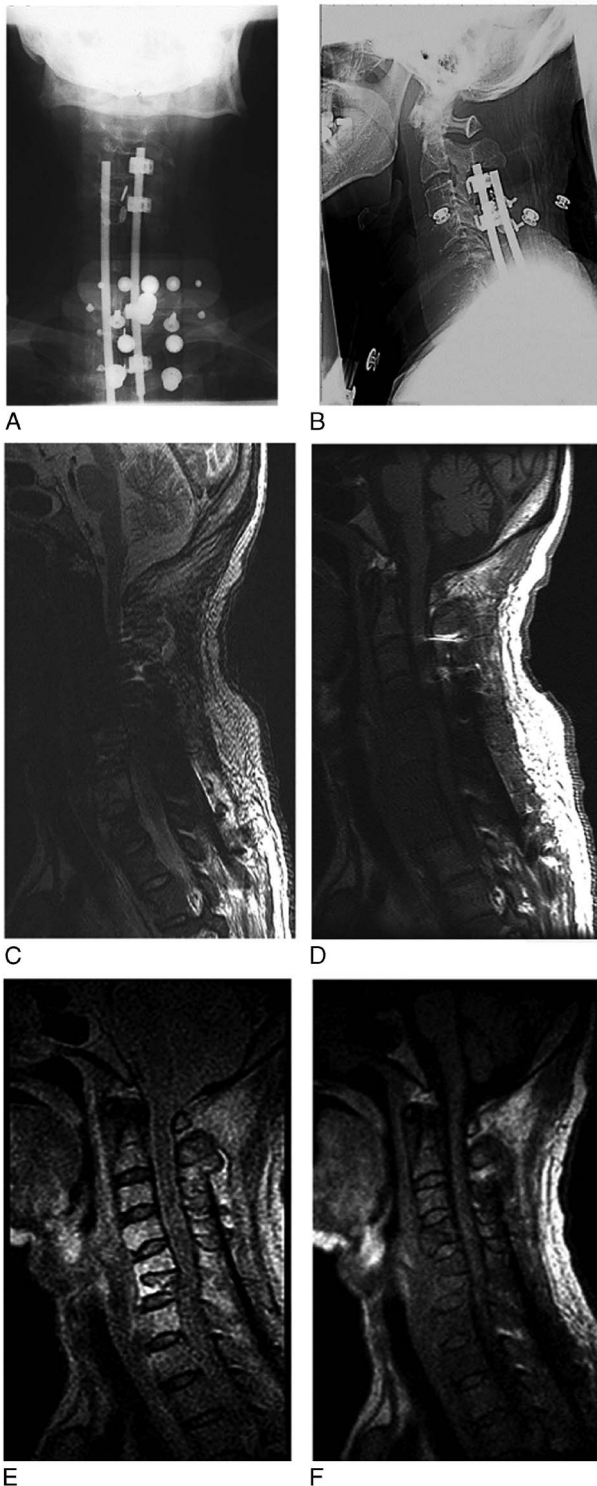
FIGURE 1. Postsurgical operative status for cervical spondylosis. Cervical radiographs show the postsurgical fixation of cervical vertebrae and the presence of metallic fixation devices (A and B). Sagittal transverse (T2) and longitudinal relaxation (T1)-weighted magnetic resonance (MR) images at 1.5 T exhibit focal signal inhomogeneity, signal loss, and artifacts, thus making it difficult to evaluate the spinal cord (C and D). Sagittal T2- and T1-weighted images reconstructed by a 0.2-T permanent magnet MR system show little image distortion or signal loss, and the spinal cord can thus be evaluated.
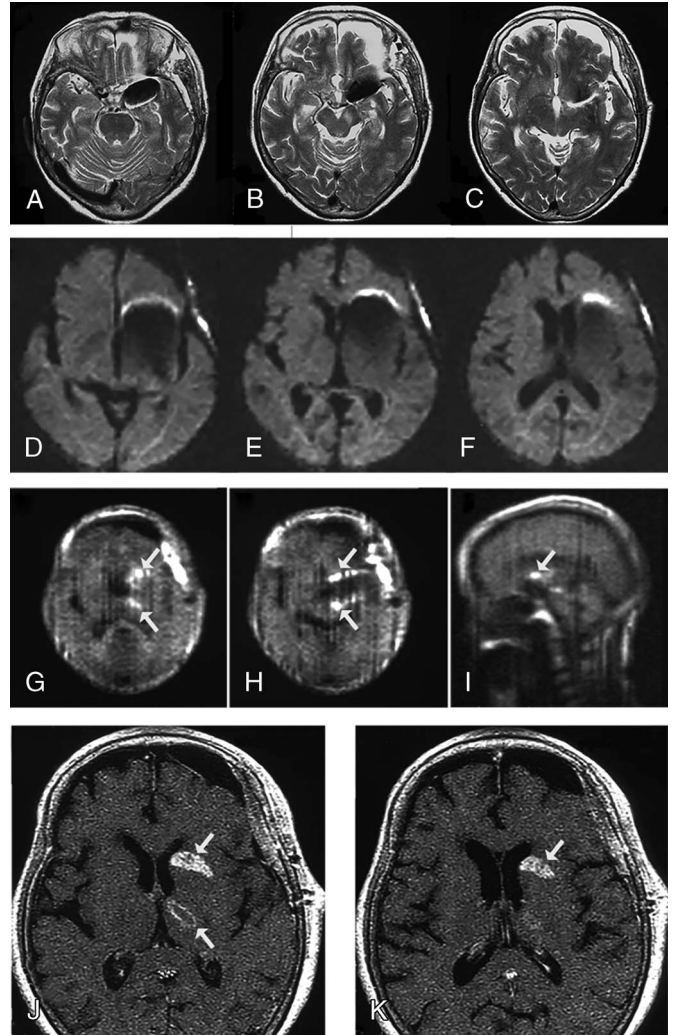

FIGURE 2. Status of the cerebral aneurysm after a neurosurgical operation. T2-weighted MR images (A–C) and diffusion-weighted images (D–F) at 1.5 T show conspicuous signal loss around the coil and metal artifacts. Evaluation of the surrounding brain parenchyma is difficult. Line-scan diffusion-weighted images (spin echo–based sequence) (G–I) at 0.2 T show an abnormally high intensity in the left caudate nucleus indicative of a recent cerebral infarction. Moreover, postcontrast-enhanced T1-weighted images (J and K) at 0.2 T show abnormal enhancements. These findings also support the assertion for the presence of a recent cerebral infarction.

is sufficient for diagnosis.[29] This indicates that, at lower field strengths, the water and fat spectra are closer to each other. Consequently, it becomes more difficult to use fat suppression pulses. In fact, the spectral width of water is broadened in a manner that is inversely proportional to the transverse relaxation star ($T2^*$), and a small nonuniformity in the magnetic field can easily suppress the water signal. Therefore, fat-suppressed imaging with CHESS (chemical shift selective), especially in low-field MRI systems (up to 0.3 T), is considered challenging.[30–32]

The short tau inversion recovery (STIR) method has been extensively used in low-field MRI systems, especially for the imaging of the bone and soft tissue area, because it achieves fat suppression with the use of a nonselective frequency technique and because the nonuniformity of the magnetic field does not constitute a problem.[33,34] However, as is well known, STIR is not recommended for use as a fat-suppressed T1-weighted image after contrast material injection because STIR suppresses both fat and any other substance with a T1 value equivalent to

that of fat.[35,36] The so-called water image in the Dixon technique may be useful as a fat-suppressed T1-weighted image after contrast enhancement.[37,38]

Moreover, the angular speed ω is proportional to the static magnetic field strength, and the correct echo time (TE) for the phase difference is inversely proportional to ω. Thus, at higher static magnetic field strengths, the appropriate value of TE is shortened. It is approximately equal to 2.3 milliseconds at 3 T, 4.6 milliseconds at 1.5 T, and 23 milliseconds at 0.3 T.[39] Therefore, methods such as in-phase/out-of-phase imaging, which are used to diagnose adrenal adenomas in the adrenal glands,[40,41] are generally difficult to achieve with low-field MRI systems. In MRI systems (field strengths ≤0.3 T), the TEs of the in-phase and out-of-phase images are considerably different, and thus result in different contrasts. It is often difficult to determine whether the difference in signal between the 2 images is attributed to fat content or TE differences. Note that the limitations in the choice of imaging methods and the differences in contrast owing to these physical characteristics are attributed to the static magnetic field strength itself, which cannot be easily overcome, even with advances in imaging technology.[42]

FIELD DEPENDENCE OF T1 VALUE

The T1 values of water protons vary as a function of the static magnetic field strength. Although there are differences between different parts of the living tissue,[43] the dependence of T1 on static magnetic field changes are attributed to the different proportions of bound water in the tissue.[44] The lower the static magnetic field strength is, the shorter is the T1 value. T1 exhibits a power-law dependence with the static field strength (ie, it is proportional to $[Bo]^{0.3}$).[45] Therefore, measured T1 values of the tissues (ie, brain) will approximately double as the field strength is increased from 0.3 T to 3.0 T.[43] This is advantageous for T1-weighted images obtained from low-field systems. In other words, the differences in T1 values in various tissues (eg, white matter and gray matter in the brain) are larger, thus resulting in better images with greater tissue contrast.[46]

GADOLINIUM-BASED CONTRAST AGENT

Gadolinium (Gd)-based contrast agents enhance tissue contrast by shortening the T1 relaxation time. The degree of T1 shortening, or relaxivity r1, induced by Gd and tissue contrast before contrast agent administration both determine the tissue contrast after contrast agent administration and depend on the field strength. Rinck and Muller[47] revealed that the contrast between white matter and glioblastoma after contrast agent administration is generally lower at lower field strengths. Although r1 is higher at lower field strengths, inherently short relaxation times of target tissues at low field strength have a higher effect on target tissue contrast after contrast agent administration. The adjustment of pulse sequence parameters and dosage or type of contrast agent according to field strength might be beneficial to achieve the optimal enhancement of target lesions. Notably, contrast enhancement at low field using double dose (0.2 mmol/kg) of intravenous Gd-based contrast agent has been reported to be similar to that at 1.5 T using standard dose (0.1 mmol/kg) in a brain study.[48] Lower contrast enhancement at low field can be problematic, especially for detecting small brain metastases[49] and checking the enhancement of multiple sclerosis lesions.[50]

SUSCEPTIBILITY EFFECT

The degradation of image quality associated with the effect of magnetic susceptibility is generally reduced at a lower static magnetic field strength.[51,52] At the boundary between tissues with significantly different magnetic susceptibilities (eg, soft tissue, bone, and air), signal degradation is observed, but it is mitigated when the static magnetic field strength is low.[51] Therefore, it may be possible to evaluate clinically lung lesions that are difficult to image at 1.5 T or 3 T with a low-field MRI system (this is discussed in more detail later).
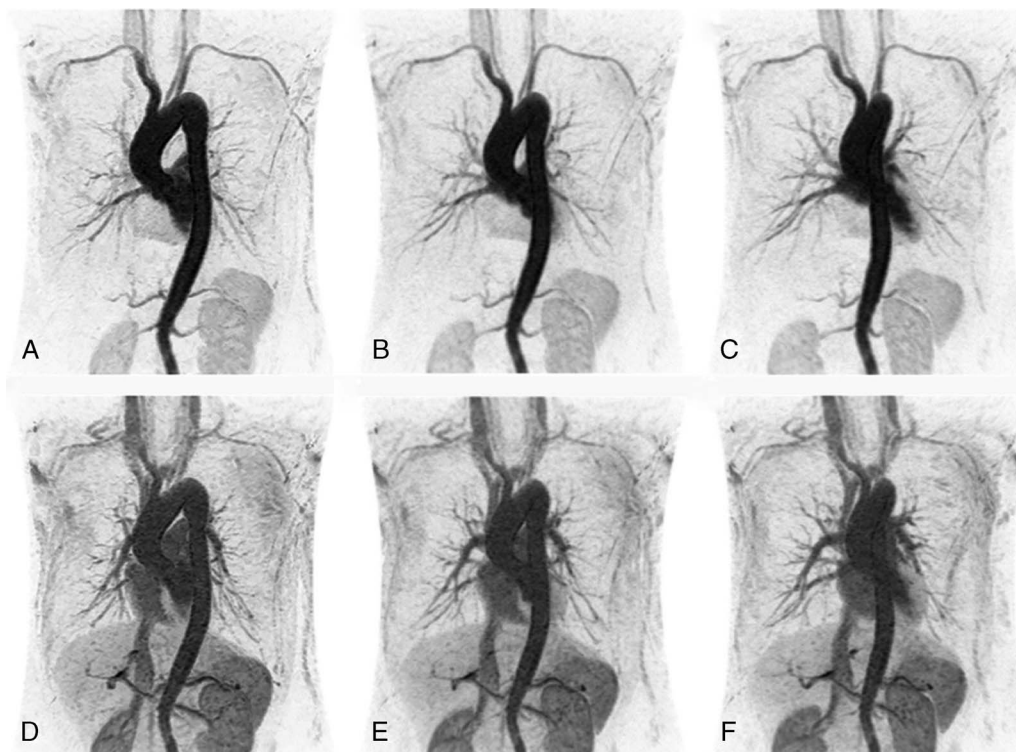

FIGURE 3. Contrast-enhanced MR angiography (MRA) of large vessels in a 0.2-T MRI system. First phase (A) and second phase (B). The sequence is efgre3d (TR/TE = 12.6/3.2 milliseconds). Voxel dimensions were 0.6 × 1.6 × 1.6 mm^3, and intravenous gadolinium contrast media were injected at a rate of 5 mL/s.
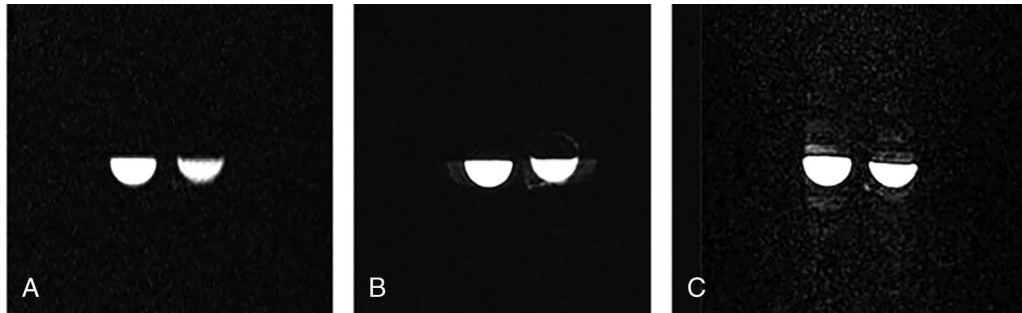
FIGURE 4. Axial images of water and an acetone phantom were obtained via diffusion-weighted imaging with a line-scan diffusion-weighted imaging (LSDWI) sequence with a b-value of 0 s/mm² (A), fast spin echo sequence (B), and multishot EPI sequence with a b-value of 0 s/mm² (C) at 0.2 T. Fewer artifacts are observed in image (A). Artifacts generated owing to the sequence design are prominent in (B) (ghosting artifacts) and (C) (image distortions). These images are associated with potential errors (reproduced with permission from Hori et al[82]).
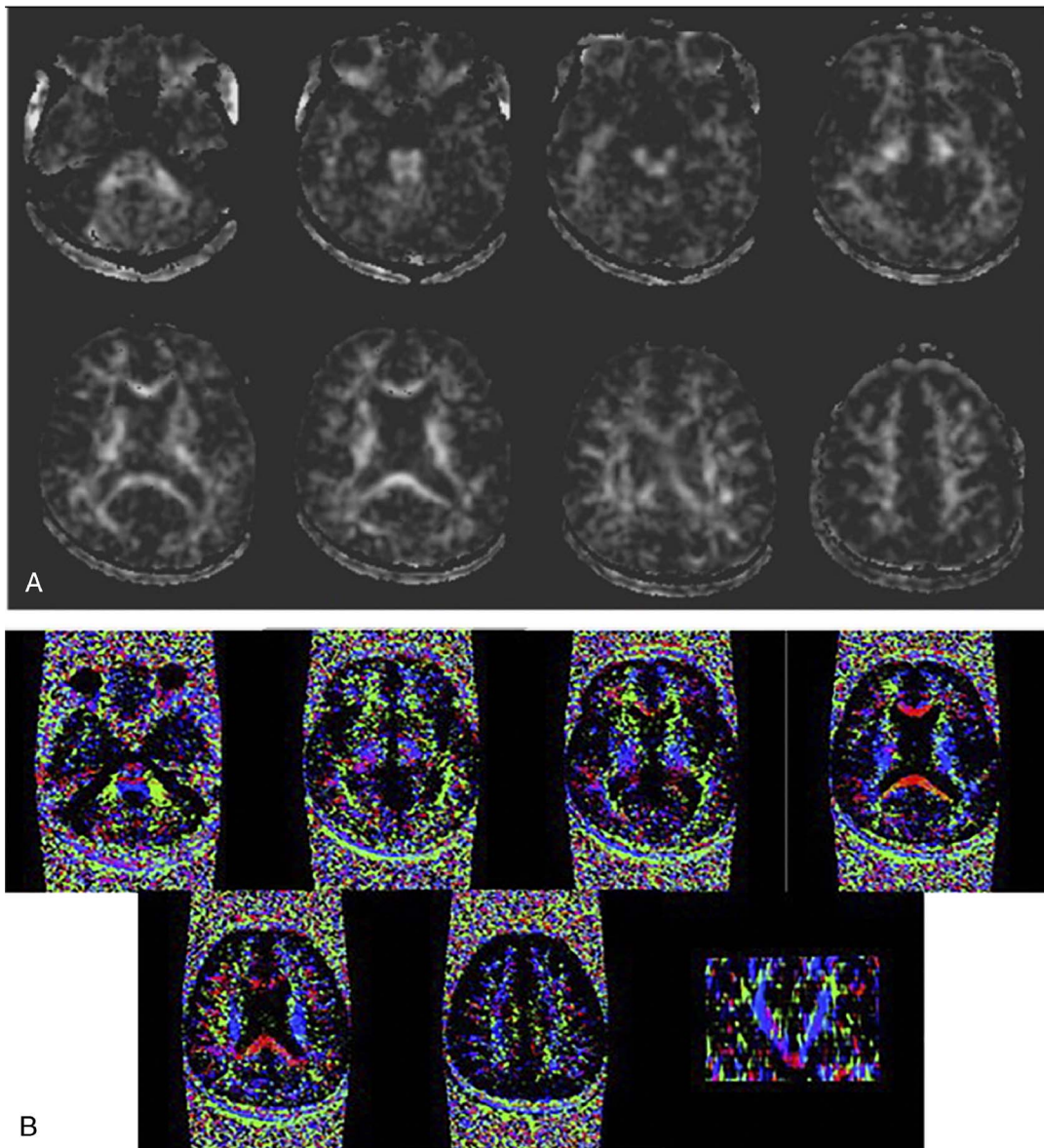
FIGURE 5. Fractional anisotropy map (A) in axial plane and color schemes (B) used to represent the orientations of anisotropic tissues in axial and coronal images obtained in a healthy volunteer by LSDWI on a 0.2-T MR scanner. The coronal image was obtained by reformatting the axial slice. In the color maps, red denotes right and left, green denotes anterior and posterior, and blue denotes the superior and inferior directions. The image quality is sufficient to estimate white matter in the brain (reproduced with permission from Hori et al[90]).

Furthermore, image degradation caused by metal implants is a problem in clinical MRI systems.[53] The magnitude of the effect on image degradation varies depending on the material constituting the metal.[54] Specifically, inadvertent imaging of a living body containing a metal implant in a 1.5-T or 3-T MRI system can cause physical traction or unacceptable heat generation in the body, thus making the examination itself potentially dangerous.[55–57] This heat generation is controlled to values accounted by the average specific absorption rate. However, it should also be noted that localized heat generation above the limit can be induced by metal implants.[58] As the force on implants is greater at high magnetic fields, the damage caused by accidental adsorption of oxygen cylinders, or other similar events, will naturally be greater at higher magnetic field strengths.[59,60] This risk is expected to be much lower for low-field MRI systems, especially those below 0.5 T. In addition, the degradation of image quality is essential for metal implants placed in living bodies (eg, clips for brain aneurysm surgery or fixtures in the orthopedic field) associated with medical procedures,[57] even in cases after imaging optimization, such as cases associated with the modification of the phase direction and TE shortening and those officially approved for imaging with MRI, regardless of the magnetic field strength.

The loss or degradation of signals in MRI scans is more severe at higher field strengths, which can impair the disease diagnosis.[61] This is an inherent advantage of a low-field MRI system. This is attributed to the fact that, if it is not useful for medical diagnosis owing to image degradation or artifacts, it is ultimately meaningless to use it (Figs. 1, 2). Regarding peripheral nerve stimulation induced by gradient switching, thermal effects by the radiofrequency field, forces, and the developed torque by the static magnetic field render the low-magnetic field system superior in terms of safety in conducting the test.[62,63]

TECHNICAL REQUIREMENTS

In general, low-field MRI systems do not require as much space and are more lightweight than the 1.5-T and 3-T MRI systems that are widely used in clinical practice. Commercial low-field MRI systems can be installed in a minimum area of 9 m^2, but the floor needs to withstand at least 1.05 tons.[1] In contrast, a high-field MRI system is a minimum of 3 tons.[64] Thus, the installation requirements of the low-field MRI system are more flexible than those of 1.5-T and 3-T MRI systems, which require multiple independent rooms (examination rooms, work rooms, and the technical room with power electronics).[2] It is easier to install and use the low-field MRI in operating rooms, emergency units, and interventional rooms. Unlike high-field MRI systems, the magnets used in low-field MRI systems are either permanent magnets[65–67] or electromagnets.[68] The former do not require power to generate the magnetic field (B0), but the latter usually have a higher field uniformity. Some MRI systems using electromagnets require simple water-cooling, but, in any case, complex and expensive cryogenics are not necessary for cooling. Being cryogen-free also eliminates the need for the quench pipe, which contributes to the flexibility of the installation space.[11] Moreover, MRI systems with a low field strength, particularly permanent magnets, have low energy consumption,[23] and therefore, they can be said to be highly energy efficient.

IN VIVO APPLICATIONS FROM THE PAST TO THE PRESENT

Contrast-Enhanced Magnetic Resonance Angiography

T1-, T2-, and T2*-weighted images and STIR are the most commonly used imaging sequences in low-field MRI systems. It was often assumed that more advanced imaging techniques are difficult to use, especially at static field strengths below 0.5 T. In addition to noncontrast MRA, such as the time-of-flight MRA, contrast-enhanced MRA using a Gd contrast agent can be imaged on low-field MR scanners.[69,70] Rinck and Muller[47] reported that the contrast effect of contrast agents in low-field MRI systems is lower than that in high-field MRI systems, which seems to be a disadvantage. However, one of the most important

FIGURE 6. A 21-year-old woman with some clinical cervical myelopathy. Sagittal reformatted 3D FIESTA (TR = 13.2 milliseconds, TE = 6.6 milliseconds) image (A), apparent diffusion coefficient (isoADC) map (B), and fractional anisotropy map (C) at 0.2 T. Note that the diameter of the cervical spinal cord on each image is different. Cerebrospinal fluid contamination in the voxel of the spinal cord may induce this phenomenon (reproduced with permission from Hori et al[82]). FIESTA (A) provides high signal-to-noise and good soft tissue image contrast for imaging because it is imaged in 3D, and spin echo–based LSDWI, imaged in the direct sagittal section, can provide distortion-free quantitative maps.
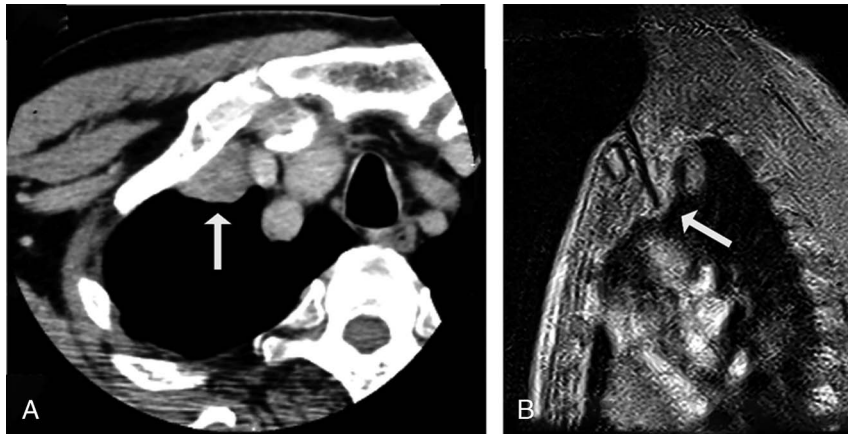
FIGURE 7. A mediastinal tumor case of an 80-year-old man. In the transverse computed tomography (CT) image, the lesion of interest is very close to the clavicle, and a safe biopsy approach would be difficult to accomplish on this image (A). Using the sagittal MRI scan, it was possible to perform biopsy with an MRI-guided approach from above with a 0.2-T MR system. The low signal region (along the indicated line) denotes the biopsy needle. Note that with the recent advanced interventional CT tool, the same procedure can be performed, but under MR guidance, ionizing radiation can be avoided.

imaging parameters for contrast-enhanced MRA is sufficiently short TE. In the past, low-field MRI systems were able to achieve the short TE required for contrast-enhanced MRA (Fig. 3). Moreover, with the improved gradient systems available nowadays, TE can be shortened even further, thus allowing the pursuit of contrast-enhanced MRA with better image quality, including higher spatial and temporal resolution.

Diffusion-Weighted Imaging

Diffusion-weighted imaging (DWI) is a technique used to visualize the mobility of water molecules in MRI. It is an important imaging technique used clinically to detect acute stroke[71–73] and to evaluate cancer.[74–78] Diffusion-weighted imaging is currently part of the clinical imaging routine in many institutions, especially for the brain, and is now being applied to the imaging of the entire body.[79–81] In the 1990s and 2000s, low-field MRI systems were not as powerful as 1.5-T MRI systems in terms of gradients. Therefore, it was difficult to use single-shot echo planar imaging (EPI), which is the most commonly used method for high-field strength MRI. Even if this was technically possible, its clinical utility was questionable because of its low spatial resolution and SNR response characteristics (Fig. 4).

However, single-shot EPI is not the only imaging technique for DWI, and various other methods have been proposed. Diffusion-weighted imaging with line-scan data acquisition (LSDWI)[83–89] does not require high-performance gradient hardware and can be applied at low magnetic fields because it is based on a spin echo sequence. This method requires a long imaging time (less than 1 hour for a 0.2-T permanent magnet MRI for diffusion tensor imaging), including 1 b0 image with 6 different motion-probing gradient images per slice, and 18 axial slices to cover the entire brain (Fig. 5).[90] If only a trace image can be obtained, the imaging time can be reduced further. Moreover, unlike EPI, the distortion is less prominent and there are fewer magnetic susceptibility artifacts; moreover, it can be performed independently of gradient strength.
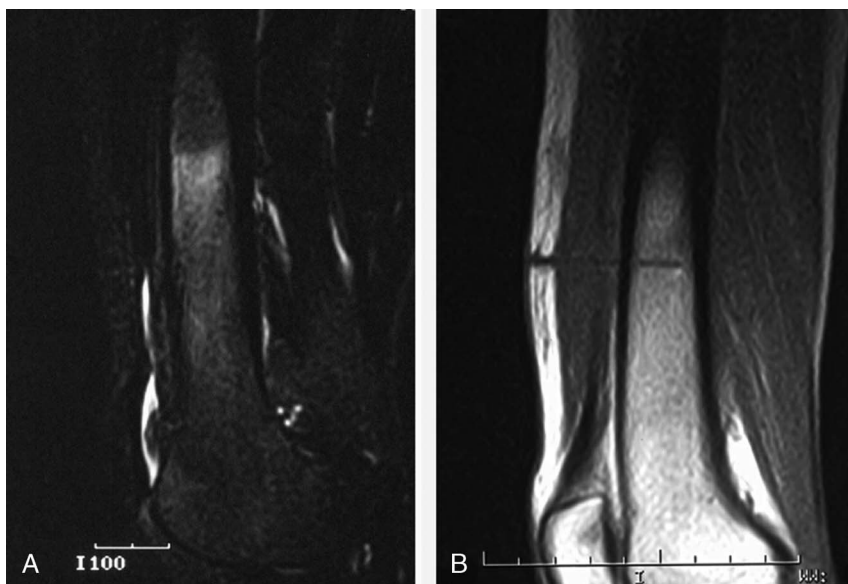

FIGURE 8. Bone scintigraphy shows multiple abnormal accumulations in the bone (not shown), and the STIR image at 0.2 T showed high signal in the intraosseous lesion. Given that it was difficult to identify the position by CT, the biopsy was performed with MRI guidance at 0.2 T using the spin echo T1-weighted sequence. This lesion was later found to be osteomyelitis.
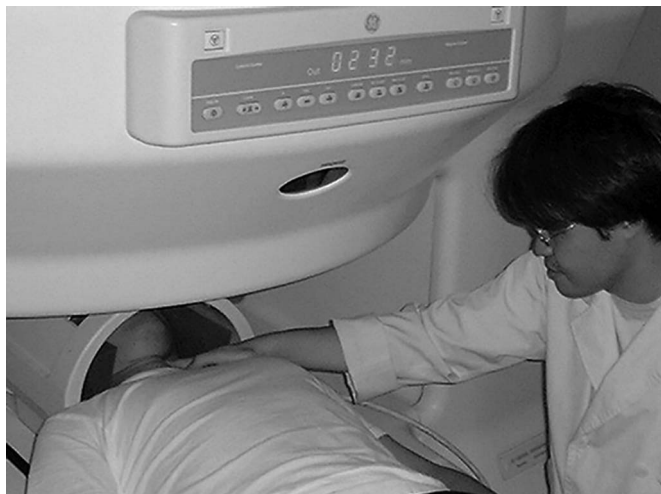
FIGURE 9. In the MR Matas test, a neuroradiologist manually compresses the common carotid artery of the affected side during scanning (reproduced with permission from Hori et al[93]).

In addition, given that this is a spin echo–based sequence, the coronal and sagittal images exhibit less distortion. Furthermore, if the number of slices is reduced in consideration of the anatomical structure, imaging can be performed in a realistic acquisition time. In fact, a study of patients with cervical spondylosis quantified and evaluated the apparent diffusion coefficient and fractional anisotropy (FA) with LSDWI of the cervical spinal cord in sagittal section within 6 minutes 18 seconds (Fig. 6).[82] However, for advanced diffusion MRI that requires multiple MPG axes, or diffusion MRI that requires many slices covering a wide range of the body (eg, cancer staging), LSDWI with its long imaging time is not an efficient imaging

method and is not recommended. Furthermore, at least on the latest 0.55-T MRI systems, the image quality of diffusion-weighted images with single-shot EPI is comparable to that of 1.5 T, with less distortion at 0.55 T than at 1.5 T.[11]

Interventional Magnetic Resonance Imaging

Low-field MRI systems are often implemented in the so-called open-type system configurations. These system types have added clinical advantages, including the fact that they deal with claustrophobia patients, and allow parental presence in pediatric patient scans. They also possess technical advantages that make interventional MRI possible. In the evaluation of these systems, the first aspect that needs to be considered is the image-guided technique, especially in the bone and soft tissue areas. In the bone and soft tissues, orthopedic procedures are usually performed under x-ray fluoroscopic guidance; however, it is often difficult to determine the exact anatomical location of soft tissues (muscles, ligaments, neoplastic lesions, etc). In contrast, MRI provides high tissue-to-tissue contrast for these, thus its usefulness in orthopedic procedures is promising.[91] Although biopsies in the field of orthopedics are also extensively performed with computed tomography (CT) guidance, we believe that soft tissue biopsies at locations that are difficult to be biopsied with CT, or those that cannot be accurately identified, are good target applications for MRI-guided techniques (Figs. 7, 8). In addition, a system for real-time tracking of the position of biopsy needle tips and catheter tips in interventional MRI in low-field MRI systems was devised in 1999.[92] Current advanced 0.55-T MRI systems allow cardiac catheterization under real-time MRI fluoroscopy guidance.[18]

Moreover, we have performed the MR Matas test by using a form of contrast-enhanced MRA, 2-dimensional MR digital subtraction angiography, and temporary manual occlusion of the affected common carotid artery by taking advantage of the characteristics of the open-type 0.2-T MR system (Fig. 9).[93] The purpose of this procedure was to complete the conventional Matas test, which requires x-ray exposure,
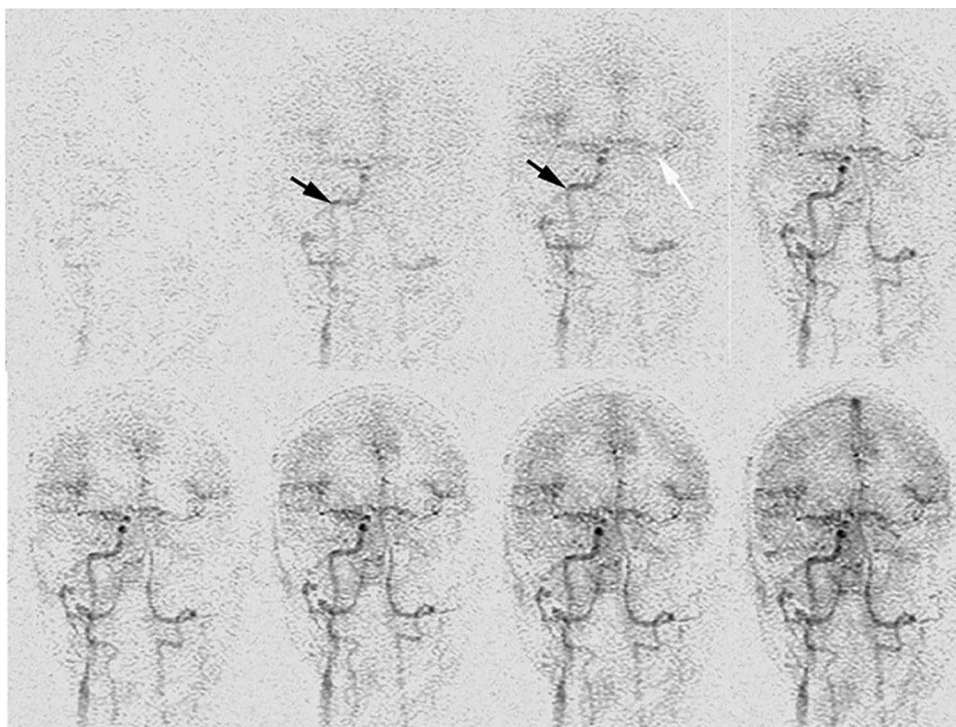
FIGURE 10. A 65-year-old man with hypopharyngeal cancer in the left side, and consequent changes to the left cerebral circulation. The left common carotid artery was compressed manually and sufficiently to stop its blood flow. The MR Matas test at 0.2 T clearly demonstrates the cross-flow from the patient side (right, black arrow) to the occluded side (left, white arrow) via the circle of Willis (reproduced with permission from Hori et al[93]).

ionizing radiation, and a skilled neurointerventional radiologist; it is thus safer and easier to perform with MRI. The image quality of the MR Matas test was generally sufficient to confirm cross-flow from the patient to the occluded side in comparison with selective intra-arterial digital subtraction angiography (Fig. 10).

In addition, because of their open forms and relatively low risk of metal adsorption accidents, low-field MRI systems are also used as part of hybrid systems in surgical operating rooms,[94] radiation oncology units,[95] and radiography systems.[96]

CUTTING-EDGE TECHNOLOGY AND FUTURE PERSPECTIVE

In recent years, low-field MRI systems equipped with high-performance gradients have been developed. These systems are expected to be clinically useful. As described previously, a lower static field strength is expected to shorten T1 and reduce magnetic susceptibility artifacts. Although the SNR decreases with the static field strength, the SNR is not determined solely by the static field strength, but by various factors, such as gradient coils and pulse sequence design. Therefore, a low-field MRI system equipped with high-performance gradients has the potential to be best for both low-field and high-field MRI systems. Campbell-Washburn et al[18] showed the feasibility of 0.55 T with high-performance imaging technology in clinical use. What is notable in their report is the excellent image quality of the MRI scans, especially of the lungs, which is inherently difficult to achieve with a 1.5-T or 3-T MRI system. In another report, pneumonia associated with COVID-19 was also evaluated with the use of this 0.55-T MRI.[97,98]

Conditions, such as diffuse lung disease or focal pneumonia, which have not been evaluated by MRI in the past, deserve further evaluation by MRI in the future. Given that CT scans are extensively used to evaluate lung lesions, it would be very useful if MRI could be used to evaluate some lung lesions, especially in children,[99] to reduce x-ray exposure. It is worth mentioning that MRI-guided right heart catheterization was performed with 0.55-T MRI. This is a prerequisite for the procedure, which requires cardiac MR images of sufficient quality; furthermore, by using a spiral out acquisition, the image quality becomes comparable with that of 1.5-T MRI. Although a guidewire is required for this procedure, no complications, such as heating, were observed. This may be attributed to the positive effects of the low static magnetic field strength.

Another area that is progressing rapidly is the use of deep learning to denoise and improve the image quality of MR images for clinical use, and for the generation of quantitative maps.[100,101] Most of the research has been conducted on 1.5-T or 3-T MRI systems, but there are possible advantages associated with low-field MRI. However, there is one possible advantage of low-field MRI, namely, the fact that deep learning can be used to make the images of low-field MRI systems look more like those of 1.5-T or 3-T MRI systems (arXiv:2003.07216v2 [eess.IV], arXiv:1909.06763v1 [eess.IV]). This method is reasonably priced and can be beneficial for classical low-field MRI systems, regardless of the model. It is expected that a method that can remove noise will be useful. However, there are some limitations to the actual clinical application of this technique. For example, as shown previously, the difference in image contrast based on physical properties caused by differences in static magnetic fields should be considered. In addition, it is not always the case that the contrast of MRI scans from a low-field MRI system is inferior to that of a high-field MRI system (eg, T1 contrast).

Furthermore, in some clinically important areas, such as time-of-flight MRA and susceptibility imaging, 3 T was widely recognized very early as being the field strength of choice.[11] In contrast, with previous low-field MRI systems, these imaging techniques were difficult to use and only poor-quality images could be obtained. However, with next-generation advanced 0.55-T low-field systems, it is possible to obtain time-of-flight MRA and susceptibility-weighted imaging with completely comparable image quality (Fig. 11). Therefore, it is

important to recognize that the magnetic field strength of the MRI system itself is not directly linked to the MRI scan quality.

In addition, applications with modern acceleration techniques, such as compressed sensing SPACE,[102] simultaneous multislice, EPI,[103] and simultaneous multislice fast spin echo imaging,[104] used in 3-T MRI, are available in this low-field system. Therefore, the poor temporal resolution of imaging, which is often pointed out as a problem in low-field MRI systems, is expected to improve.

Finally, let us have a brief look at portable scanners. All of the aforementioned MRI systems are fixed-installation systems and may be
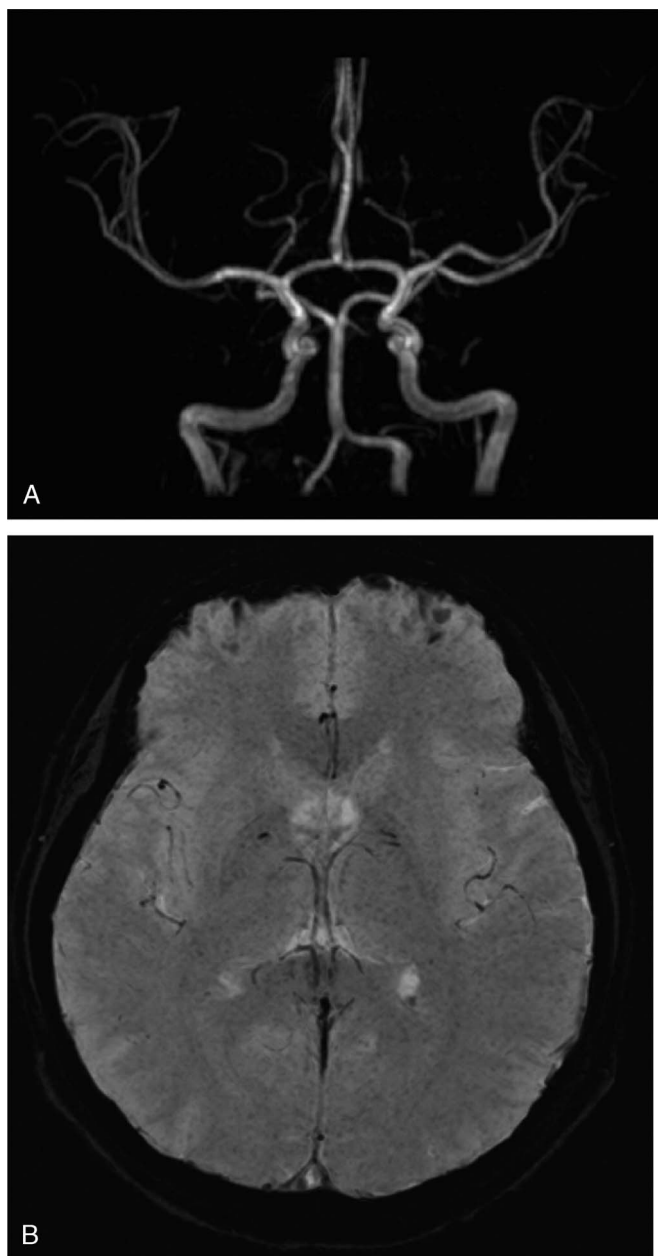
FIGURE 11. Time-of-flight MRA (A) and minimal intensity projection susceptibility-weighted imaging (B) from the recent advanced 0.55-T MRI system. Voxel dimensions were $0.5 \times 0.5 \times 0.5$ mm^3 in time-of-flight MRA and $0.3 \times 0.3 \times 16.0$ mm^3 in minimal intensity projection susceptibility-weighted imaging with approximate scan times of 5 and 6 minutes. Courtesy of Hiromori Uneda and Akihiro Manabe, Siemens Healthcare Japan.

difficult to access depending on the patient's condition or infrastructure requirements. Therefore, if a compact and lightweight MRI system could be realized similar to an ultrasound system, it could be expected to be clinically useful, especially in the evaluation of critically ill patients. Cooley et al[105] introduced a compact, portable MRI system for the head that uses a 122-kg low-field (80 mT) magnet,[105–107] in conjunction with actual imaging data. The spatial resolution of this system is lower, and the imaging time is longer than that of a conventional fixed MRI system. However, clinically useful images, such as T1- and T2-weighted images, have been obtained, and future developments are expected. In addition, surprisingly, MR systems that can perform routine imaging, such as T1, T2, FLAIR, and DWI in the intensive care unit, have also been developed.[108]

CONCLUSIONS

Imaging techniques and images in low-field MRI systems are currently more advanced than is commonly recognized. Since the late 1990s, various applications, such as contrast-enhanced MRA and DWI, have become possible. Moreover, it should also be understood that the physical characteristics of low-field systems make them superior to high-field MRI in many ways (eg, T1-shortening effects and low-magnetic-susceptibility artifacts associated with the static field strength). Recent advanced techniques, such as the use of powered gradients, sophisticated radiofrequency coils, and optimized sequences, have shown that the static field strength itself does not necessarily need to be high. In addition, with the recent remarkable developments in deep learning techniques, noise due to low static field strengths can be removed more effectively than before. Clinically, the fundamental value of MRI lies in tissue contrast information, which cannot be replaced by other modalities, such as CT.[109] For this reason, the strength of the static magnetic field and cost are important issues. Overall, we believe that low-field MRI systems will continue to develop and become more widespread in the future.

REFERENCES

1. Marques JP, Simonis FFJ, Webb AG. Low-field MRI: an MR physics perspective. *J Magn Reson Imaging*. 2019;49:1528–1542.
2. Sarracanie M, Salameh N. Low-field MRI: how low can we go? A fresh view on an old debate. *Front Phys*. 2020;8:172.
3. Bilaniuk LT, Zimmerman RA, Wehrli FW, et al. Cerebral magnetic resonance: comparison of high and low field strength imaging. *Radiology*. 1984;153:409–414.
4. Hittmair K, Kramer J, Rand T, et al. Infratentorial brain maturation: a comparison of MRI at 0.5 and 1.5T. *Neuroradiology*. 1996;38:360–366.
5. Rand T, Imhof H, Turetschek K, et al. Comparison of low field (0.2T) and high field (1.5T) MR imaging in the differentiation of torned from intact menisci. *Eur J Radiol*. 1999;30:22–27.
6. Magee T, Shapiro M, Williams D. Comparison of high-field-strength versus low-field-strength MRI of the shoulder. *AJR Am J Roentgenol*. 2003;181:1211–1215.
7. Murray RC, Mair TS, Sherlock CE, et al. Comparison of high-field and low-field magnetic resonance images of cadaver limbs of horses. *Vet Rec*. 2009;165:281–288.
8. Smith MA, Dyson SJ, Murray RC. The appearance of the equine metacarpophalangeal region on high-field vs. standing low-field magnetic resonance imaging. *Vet Radiol Ultrasound*. 2011;52:61–70.
9. Przyborowska P, Adamiak Z, Holak P, et al. Comparison of feline brain anatomy in 0.25 and 3 Tesla magnetic resonance images. *Anat Histol Embryol*. 2017;46:178–186.
10. Hayashi N, Watanabe Y, Masumoto T, et al. Utilization of low-field MR scanners. *Magn Reson Med Sci*. 2004;3:27–38.
11. Runge VM, Heverhagen JT. Advocating the development of next-generation, advanced-design low-field magnetic resonance systems. *Invest Radiol*. 2020;55:747–753.
12. Yamada K, Miyahara K, Sato M, et al. Optimizing technical conditions for magnetic resonance imaging of the rat brain and abdomen in a low magnetic field. *Vet Radiol Ultrasound*. 1995;36:523–527.
13. Choquet P, Breton E, Goetz C, et al. Dedicated low-field MRI in mice. *Phys Med Biol*. 2009;54:5287–5299.
14. Ejbjerg BJ, Narvestad E, Jacobsen S, et al. Optimised, low cost, low field dedicated extremity MRI is highly specific and sensitive for synovitis and bone erosions in rheumatoid arthritis wrist and finger joints: comparison with conventional high field MRI and radiography. *Ann Rheum Dis*. 2005;64:1280–1287.
15. Iturri-Clavero F, Galbarriatu-Gutierrez L, Gonzalez-Uriarte A, et al. "Low-field" intraoperative MRI: a new scenario, a new adaptation. *Clin Radiol*. 2016;71:1193–1198.
16. Senft C, Ulrich CT, Seifert V, et al. Intraoperative magnetic resonance imaging in the surgical treatment of cerebral metastases. *J Surg Oncol*. 2010;101:436–441.
17. Senft C, Seifert V, Hermann E, et al. Surgical treatment of cerebral abscess with the use of a mobile ultralow-field MRI. *Neurosurg Rev*. 2009;32:77–84; discussion 84–85.
18. Campbell-Washburn AE, Ramasawmy R, Restivo MC, et al. Opportunities in interventional and diagnostic imaging by using high-performance low-field-strength MRI. *Radiology*. 2019;293:384–393.
19. Schukro C, Puchner SB. Safety and efficiency of low-field magnetic resonance imaging in patients with cardiac rhythm management devices. *Eur J Radiol*. 2019;118:96–100.
20. Klein HM. *Clinical Low Field Strength Magnetic Resonance Imaging*. Switzerland: Springer International Publishing; 2016.
21. Kaufman L. The impact of radiology's culture on the cost of magnetic resonance imaging. *J Magn Reson Imaging*. 1996;6:67–71.
22. Kersting-Sommerhoff B, Hof N, Lenz M, et al. MRI of peripheral joints with a low-field dedicated system: a reliable and cost-effective alternative to high-field units? *Eur Radiol*. 1996;6:561–565.
23. Klein HM. Low-field magnetic resonance imaging. *Rofo*. 2020;192:537–548.
24. Babcock EE, Brateman L, Weinreb JC, et al. Edge artifacts in MR images: chemical shift effect. *J Comput Assist Tomogr*. 1985;9:252–257.
25. Hood MN, Ho VB, Smirniotopoulos JG, et al. Chemical shift: the artifact and clinical tool revisited. *Radiographics*. 1999;19:357–371.
26. Albano D, Agnello F, Midiri F, et al. Imaging features of adrenal masses. *Insights Imaging*. 2019;10:1.
27. van Vucht N, Santiago R, Lottmann B, et al. The Dixon technique for MRI of the bone marrow. *Skeletal Radiol*. 2019;48:1861–1874.
28. Brateman L. Chemical shift imaging: a review. *AJR Am J Roentgenol*. 1986;146:971–980.
29. Smith AS, Weinstein MA, Hurst GC, et al. Intracranial chemical-shift artifacts on MR images of the brain: observations and relation to sampling bandwidth. *AJR Am J Roentgenol*. 1990;154:1275–1283.
30. Haase A, Frahm J, Hänicke W, et al. 1H NMR chemical shift selective (CHESS) imaging. *Phys Med Biol*. 1985;30:341–344.
31. Frahm J, Haase A, Hänicke W, et al. Chemical shift selective MR imaging using a whole-body magnet. *Radiology*. 1985;156:441–444.
32. Keller PJ, Hunter WW Jr., Schmalbrock P. Multisection fat-water imaging with chemical shift selective presaturation. *Radiology*. 1987;164:539–5341.
33. Meyers SP, Wiener SN. Magnetic resonance imaging features of fractures using the short tau inversion recovery (STIR) sequence: correlation with radiographic findings. *Skeletal Radiol*. 1991;20:499–507.
34. O'Connell MJ, Hargaden G, Powell T, et al. Whole-body turbo short tau inversion recovery MR imaging using a moving tabletop. *AJR Am J Roentgenol*. 2002;179:866–868.
35. Krinsky G, Rofsky NM, Weinreb JC. Nonspecificity of short inversion time inversion recovery (STIR) as a technique of fat suppression: pitfalls in image interpretation. *AJR Am J Roentgenol*. 1996;166:523–526.
36. Mirowitz SA. Fast scanning and fat-suppression MR imaging of musculoskeletal disorders. *AJR Am J Roentgenol*. 1993;161:1147–1157.
37. Ma J. Dixon techniques for water and fat imaging. *J Magn Reson Imaging*. 2008;28:543–558.
38. Ma J. A single-point Dixon technique for fat-suppressed fast 3D gradient-echo imaging with a flexible echo time. *J Magn Reson Imaging*. 2008;27:881–890.
39. Merkle EM, Nelson RC. Dual gradient-echo in-phase and opposed-phase hepatic MR imaging: a useful tool for evaluating more than fatty infiltration or fatty sparing. *Radiographics*. 2006;26:1409–1418.
40. Reinig JW, Stutley JE, Leonhardt CM, et al. Differentiation of adrenal masses with MR imaging: comparison of techniques. *Radiology*. 1994;192:41–46.
41. Savci G, Yazici Z, Sahin N, et al. Value of chemical shift subtraction MRI in characterization of adrenal masses. *AJR Am J Roentgenol*. 2006;186:130–135.
42. Wallyn J, Anton N, Akram S, et al. Biomedical imaging: principles, technologies, clinical aspects, contrast agents, limitations and future trends in nanomedicines. *Pharm Res*. 2019;36:78.
43. Stanisz GJ, Odrobina EE, Pun J, et al. T1, T2 relaxation and magnetization transfer in tissue at 3T. *Magn Reson Med*. 2005;54:507–512.

44. Escanye JM, Canet D, Robert J. Frequency dependence of water proton longitudinal nuclear magnetic relaxation times in mouse tissues at 20 degrees C. *Biochim Biophys Acta*. 1982;721:305–311.

45. Rooney WD, Johnson G, Li X, et al. Magnetic field and tissue dependencies of human brain longitudinal 1H2O relaxation in vivo. *Magn Reson Med*. 2007;57:308–318.

46. Bushberg JT, Boone JM. *The Essential Physics of Medical Imaging*. Philadelphia, PA: Wolters Kluwer Health; 2011.

47. Rinck PA, Muller RN. Field strength and dose dependence of contrast enhancement by gadolinium-based MR contrast agents. *Eur Radiol*. 1999;9:998–1004.

48. Desai NK, Runge VM. Contrast use at low field: a review. *Top Magn Reson Imaging*. 2003;14:360–344.

49. Brekenfeld C, Foert E, Hundt W, et al. Enhancement of cerebral diseases: how much contrast agent is enough? Comparison of 0.1, 0.2, and 0.3 mmol/kg gadoteridol at 0.2 T with 0.1 mmol/kg gadoteridol at 1.5 T. *Invest Radiol*. 2001;36:266–275.

50. Ertl-Wagner BB, Reith W, Sartor K. Low field-low cost: can low-field magnetic resonance systems replace high-field magnetic resonance systems in the diagnostic assessment of multiple sclerosis patients? *Eur Radiol*. 2001;11:1490–1494.

51. Morelli JN, Runge VM, Ai F, et al. An image-based approach to understanding the physics of MR artifacts. *Radiographics*. 2011;31:849–866.

52. Basar B, Sonmez M, Yildirim DK, et al. Susceptibility artifacts from metallic markers and cardiac catheterization devices on a high-performance 0.55 T MRI system. *Magn Reson Imaging*. 2021;77:14–20.

53. Hargreaves BA, Worters PW, Pauly KB, et al. Metal-induced artifacts in MRI. *AJR Am J Roentgenol*. 2011;197:547–555.

54. Koch KM, Hargreaves BA, Pauly KB, et al. Magnetic resonance imaging near metal implants. *J Magn Reson Imaging*. 2010;32:773–787.

55. Shellock FG. Biomedical implants and devices: assessment of magnetic field interactions with a 3.0-Tesla MR system. *J Magn Reson Imaging*. 2002;16:721–732.

56. Olsrud J, Lätt J, Brockstedt S, et al. Magnetic resonance imaging artifacts caused by aneurysm clips and shunt valves: dependence on field strength (1.5 and 3 T) and imaging parameters. *J Magn Reson Imaging*. 2005;22:433–437.

57. Radzi S, Cowin G, Robinson M, et al. Metal artifacts from titanium and steel screws in CT, 1.5T and 3T MR images of the tibial Pilon: a quantitative assessment in 3D. *Quant Imaging Med Surg*. 2014;4:163–172.

58. Ho HS. Safety of metallic implants in magnetic resonance imaging. *J Magn Reson Imaging*. 2001;14:472–477.

59. Colletti PM. Size "H" oxygen cylinder: accidental MR projectile at 1.5 Tesla. *J Magn Reson Imaging*. 2004;19:141–143.

60. Chaljub G, Kramer LA, Johnson RF 3rd, et al. Projectile cylinder accidents resulting from the presence of ferromagnetic nitrous oxide or oxygen tanks in the MR suite. *AJR Am J Roentgenol*. 2001;177:27–30.

61. Aboelmagd S, Malcolm P, Toms A. Magnetic resonance imaging of metal artifact reduction sequences in the assessment of metal-on-metal hip prostheses. *Rep Med Imaging*. 2014;7:65–74.

62. Stecco A, Saponaro A, Carriero A. Patient safety issues in magnetic resonance imaging: state of the art. *Radiol Med*. 2007;112:491–508.

63. Sammet S. Magnetic resonance safety. *Abdom Radiol (NY)*. 2016;41:444–451.

64. Cosmus TC, Parizh M. Advances in whole-body MRI magnets. *IEEE Trans Appl Supercond*. 2011;21:2104–2109.

65. Chen J, Wang D, Cheng S, et al. A hysteresis model based on linear curves for NdFeB permanent magnet considering temperature effects. *IEEE Trans Magn*. 2018;54:1–5.

66. Miyake T, Akai H. Quantum theory of rare-earth magnets. *J Physical Soc Japan*. 2018;87:041009.

67. Hinomura T, Nasu S, Kanekiyo H, et al. Magnetic properties of Nd–Fe–B–Cr nanocrystalline composite magnets. *Materials Transactions, JIM*. 1997;38:1106–1115.

68. Warner R, Pittard S. *Chapter 2 Magnets. Magnetic Resonance Technology: Hardware and System Component Design*. Cambridge, UK: The Royal Society of Chemistry; 2016:48–80.

69. Masumoto T, Hayashi N, Mori H, et al. Development of intraarterial contrast-enhanced 2D MRDSA with a 0.3 Tesla open MRI system. *Magn Reson Med Sci*. 2003;2:97–103.

70. Stecco A, Oronzo P, Armienti F, et al. Contrast-bolus MR angiography of the transplanted kidney with a low-field (0.5-T) scanner: diagnostic accuracy, sensitivity and specificity of images and reconstructions in the evaluation of vascular complications. *Radiol Med*. 2007;112:1026–1035.

71. van Everdingen KJ, van der Grond J, Kappelle LJ, et al. Diffusion-weighted magnetic resonance imaging in acute stroke. *Stroke*. 1998;29:1783–1790.

72. Vilela P. Acute stroke differential diagnosis: stroke mimics. *Eur J Radiol*. 2017;96:133–144.

73. Vilela P, Rowley HA. Brain ischemia: CT and MRI techniques in acute ischemic stroke. *Eur J Radiol*. 2017;96:162–172.

74. Alkanhal H, Das K, Poptani H. Diffusion- and perfusion-weighted magnetic resonance imaging methods in nonenhancing gliomas. *World Neurosurg*. 2020;141:123–130.

75. Charles-Edwards EM, deSouza NM. Diffusion-weighted magnetic resonance imaging and its application to cancer. *Cancer Imaging*. 2006;6:135–143.

76. Kan P, Liu JK, Hedlund G, et al. The role of diffusion-weighted magnetic resonance imaging in pediatric brain tumors. *Childs Nerv Syst*. 2006;22:1435–1439.

77. Schaefer PW, Grant PE, Gonzalez RG. Diffusion-weighted MR imaging of the brain. *Radiology*. 2000;217:331–345.

78. Usuda K, Funazaki A, Maeda R, et al. Economic benefits and diagnostic quality of diffusion-weighted magnetic resonance imaging for primary lung cancer. *Ann Thorac Cardiovasc Surg*. 2017;23:275–280.

79. Godinho MV, Lopes FPPL, Costa FM. Whole-body magnetic resonance imaging for the assessment of metastatic breast cancer. *Cancer Manag Res*. 2018;10:6743–6756.

80. Lee K, Park HY, Kim KW, et al. Advances in whole body MRI for musculoskeletal imaging: diffusion-weighted imaging. *J Clin Orthop Trauma*. 2019;10:680–686.

81. Yoshida S, Takahara T, Arita Y, et al. Whole-body diffusion-weighted magnetic resonance imaging: diagnosis and follow up of prostate cancer and beyond. *Int J Urol*. 2021;28:502–513.

82. Hori M, Okubo T, Aoki S, et al. Line scan diffusion tensor MRI at low magnetic field strength: feasibility study of cervical spondylotic myelopathy in an early clinical stage. *J Magn Reson Imaging*. 2006;23:183–188.

83. Robertson RL, Ben-Sira L, Barnes PD, et al. MR line-scan diffusion-weighted imaging of term neonates with perinatal brain ischemia. *AJNR Am J Neuroradiol*. 1999;20:1658–1670.

84. Robertson RL, Maier SE, Robson CD, et al. MR line scan diffusion imaging of the brain in children. *AJNR Am J Neuroradiol*. 1999;20:419–425.

85. Robertson RL, Maier SE, Mulkern RV, et al. MR line-scan diffusion imaging of the spinal cord in children. *AJNR Am J Neuroradiol*. 2000;21:1344–1348.

86. Maier SE, Bogner P, Bajzik G, et al. Normal brain and brain tumor: multicomponent apparent diffusion coefficient line scan imaging. *Radiology*. 2001;219:842–849.

87. Mamata H, Mamata Y, Westin CF, et al. High-resolution line scan diffusion tensor MR imaging of white matter fiber tract anatomy. *AJNR Am J Neuroradiol*. 2002;23:67–75.

88. Maier SE, Mamata H. Diffusion tensor imaging of the spinal cord. *Ann N Y Acad Sci*. 2005;1064:50–60.

89. Mamata H, Jolesz FA, Maier SE. Apparent diffusion coefficient and fractional anisotropy in spinal cord: age and cervical spondylosis-related changes. *J Magn Reson Imaging*. 2005;22:38–43.

90. Hori M, Aoki S, Okubo T, et al. Line-scan diffusion tensor MR imaging at 0.2 T: Feasibility study. *J Magn Reson Imaging*. 2005;22:794–798.

91. Petersilge CA, Lewin JS, Duerk JL, et al. MR arthrography of the shoulder: rethinking traditional imaging procedures to meet the technical requirements of MR imaging guidance. *AJR Am J Roentgenol*. 1997;169:1453–1457.

92. Aoki S, Nanbu A, Araki T, et al. Active MR tracking on a 0.2 Tesla MR imager. *Radiat Med*. 1999;17:251–257.

93. Hori M, Okubo T, Aoki S, et al. The magnetic resonance matas test: feasibility and comparison with the conventional intraarterial balloon test occlusion with SPECT perfusion imaging. *J Magn Reson Imaging*. 2005;21:709–714.

94. Schulder M, Carmel PW. Intraoperative magnetic resonance imaging: impact on brain tumor surgery. *Cancer Control*. 2003;10:115–124.

95. Mutic S, Dempsey JF. The ViewRay system: magnetic resonance-guided and controlled radiotherapy. *Semin Radiat Oncol*. 2014;24:196–169.

96. Freeman-Walsh CB, Fahrig R, Ganguly A, et al. A hybrid radiography/MRI system for combining hysterosalpingography and MRI in infertility patients: initial experience. *AJR Am J Roentgenol*. 2008;190:W157–W160.

97. Campbell-Washburn AE, Suffredini AF, Chen MY. High-performance 0.55-T lung MRI in patient with COVID-19 infection. *Radiology*. 2021;299:E246–E247.

98. Heiss R, Grodzki DM, Horger W, et al. High-performance low field MRI enables visualization of persistent pulmonary damage after COVID-19. *Magn Reson Imaging*. 2021;76:49–51.

99. Nozawa K, Niwa T, Aida N. Imaging of cystic lung lesions in infants using pointwise encoding time reduction with radial acquisition (PETRA). *Magn Reson Med Sci*. 2019;18:299–300.

100. Kawamura M, Tamada D, Funayama S, et al. Accelerated acquisition of high-resolution diffusion-weighted imaging of the brain with a multi-shot

echo-planar sequence: deep-learning-based denoising. *Magn Reson Med Sci.* 2021;20:99–105.

101. Tachibana Y, Hagiwara A, Hori M, et al. The utility of a convolutional neural network for generating a myelin volume index map from rapid simultaneous relaxometry imaging. *Magn Reson Med Sci.* 2020;19:324–332.

102. Matcuk GR, Gross JS, Fields BKK, et al. Compressed sensing MR imaging (CS-MRI) of the knee: assessment of quality, inter-reader agreement, and acquisition time. *Magn Reson Med Sci.* 2020;19:254–258.

103. Xu J, Moeller S, Auerbach EJ, et al. Evaluation of slice accelerations using multiband echo planar imaging at 3 T. *Neuroimage.* 2013;83:991–1001.

104. Murata S, Tachibana Y, Murata K, et al. Comparison of magnetization transfer contrast of conventional and simultaneous multislice turbo spin echo acquisitions focusing on excitation time interval. *Jpn J Radiol.* 2019;37:579–589.

105. Cooley CZ, McDaniel PC, Stockmann JP, et al. A portable scanner for magnetic resonance imaging of the brain. *Nat Biomed Eng.* 2021;5:229–239.

106. Wald LL, McDaniel PC, Witzel T, et al. Low-cost and portable MRI. *J Magn Reson Imaging.* 2020;52:686–696.

107. Mateen FJ, Cooley CZ, Stockmann JP, et al. Low-field portable brain MRI in CNS demyelinating disease. *Mult Scler Relat Disord.* 2021;51:102903.

108. Turpin J, Unadkat P, Thomas J, et al. Portable magnetic resonance imaging for ICU patients. *Crit Care Explor.* 2020;2:e0306.

109. Bhat SS, Fernandes TT, Poojar P, et al. Low-field MRI of stroke: challenges and opportunities. *J Magn Reson Imaging.* 2020;e27324.